Translational Oncology
www.transonc.com

Volume 7 Number 2 April 2014 pp. 240–247 240

^{18}F-Fluorodeoxyglucose Uptake and Tumor Hypoxia: Revisit ^{18}F-Fluorodeoxyglucose in Oncology Application

Xiao-Feng Li*,†, Yang Du‡, Yuanyuan Ma§, Gregory C. Postel* and A. Cahid Civelek*

*Department of Diagnostic Radiology, School of Medicine, University of Louisville, Louisville, KY, USA; †Department of Medical Physics, Memorial Sloan-Kettering Cancer Center, New York, NY, USA; ‡Laboratory of Molecular Imaging, Institute of Automation, Chinese Academy of Sciences, Beijing, China; §Department of Pathology, Memorial Sloan-Kettering Cancer Center, New York, NY, USA

Abstract

This study revisited ^{18}F-fluorodeoxyglucose (^{18}F-FDG) uptake and its relationship to hypoxia in various tumor models. *METHODS*: We generated peritoneal carcinomatosis and subcutaneous xenografts of colorectal cancer HT29, breast cancer MDA-MB-231, and non–small cell lung cancer A549 cell lines in nude mice. The partial oxygen pressure (pO_2) of ascites fluid was measured. ^{18}F-FDG accumulation detected by digital autoradiography was related to tumor hypoxia visualized by pimonidazole binding and glucose transporter-1 (GLUT-1) in frozen tumor sections. *RESULTS*: Ascites pO_2 was 0.90 ± 0.53 mm Hg. Single cancer cells and clusters suspended in ascites fluid as well as submillimeter serosal tumors stained positive for pimonidazole and GLUT-1 and had high ^{18}F-FDG uptake. In contrast, ^{18}F-FDG uptake was significantly lower in normoxic portion (little pimonidazole binding or GLUT-1 expression) of larger serosal tumors or subcutaneous xenografts, which was not statistically different from that in the liver. *CONCLUSIONS*: Glucose demand (^{18}F-FDG uptake) in severely hypoxic ascites carcinomas and hypoxic portion of larger tumors is significantly higher than in normoxic cancer cells. Warburg effect originally obtained from Ehrlich ascites carcinoma may not apply to normoxic cancer cells. Our findings may benefit the better understanding of ^{18}F-FDG PET in oncology application.

Translational Oncology (2014) 7, 240–247

Introduction

German biologist Otto Warburg, who hypothesized that even in the presence of ample oxygen, cancer cells prefer to metabolize glucose by "aerobic glycolysis" due to mitochondrial dysfunction, the so-called Warburg effect, found that Ehrlich ascites carcinoma cancer cells had increased glucose demand [1]. Increased glucose demand is considered as one of the fundamental features of cancer [2], and it has been exploited clinically for cancer detection by ^{18}F-fluorodeoxyglucose (^{18}F-FDG, an analog of glucose) positron emission tomography (PET).

According to the Warburg effect, aerobic glycolysis would confer a general increase in ^{18}F-FDG uptake throughout all viable cancer cells of the tumors, spatially unrelated to oxygen status. However, growing evidence has demonstrated that intratumoral ^{18}F-FDG distribution is highly heterogeneous and may be hypoxia dependent. Hypoxic cancer cells have significantly higher radiolabeled FDG uptake in *in vitro* [3-6] and in *in vivo* animal studies [7-9]. While high ^{18}F-FDG uptake is observed in most patients by PET/computed tomography (CT), ^{18}F-FDG–negative solid malignancies are frequently found [10,11]. In a clinical study of primary and metastatic non–small cell lung cancers (NSCLCs), regions of tumor with high levels of angiogenesis associated with low ^{18}F-FDG uptake were reported [12]. The ^{18}F-FDG data suggest that hypoxic cancer cells need more glucose than normoxic cancer cells for biology process.

Warburg used Ehrlich ascites cells because they were almost pure cultures of cancer cells with which one can work quantitatively as in chemical analysis, in contrast to solid tumors with a mixture of

Address all correspondence to: Xiao-Feng Li, MD, PhD, Department of Diagnostic Radiology, School of Medicine, University of Louisville, 530 South Jackson Street, CCB-C07, Louisville, KY 40202. E-mail: Linucmed@gmail.com
Received 10 December 2013; Revised 2 January 2014; Accepted 15 January 2014

http://dx.doi.org/10.1016/j.tranon.2014.02.010

components. Ehrlich ascites cells were assumed as in ample oxygen condition [21% O_2 or partial oxygen pressure (pO_2) = 160 mm Hg].We recently reported that single cancer cells and clusters of cancer cells suspended in ascites fluid were extensively hypoxic [13-15], while hypoxia is defined as pO_2 less than 10 mm Hg or 1.3% O_2. In this study, we directly measured the pO_2 of ascites fluid using OxyLite technology; the presence of hypoxia in ascites tumors was demonstrated by immunohistochemical visualization of exogenous and endogenous hypoxia markers, and glucose demand in ascites tumors was evaluated and measured by ^{18}F-FDG uptake. Our findings demonstrated that the pO_2 in ascites fluid was very low, and both single cancer cells and cell clusters suspended therein were severely hypoxic. Moreover, hypoxic cancer cells had higher ^{18}F-FDG uptake than normoxic cancer cells.

Materials and Methods

Cancer Cell Lines and Animals

Three different human cancer cell lines were used in the experiments: colon cancer HT29, breast cancer MDA-MB-231, and NSCLC A549. Cells were maintained in McCoy's 5A modified medium, RPMI 1640, and F-12K medium, respectively. All media were supplemented with 10% FBS, 1% glutamine, and 1% antibiotic mixture. Cells were grown at 37°C in a humidified 5% CO_2 incubator. Exponentially growing cells were harvested with 0.25% (wt/vol) trypsin–0.53 mM EDTA solution, washed, and suspended in phosphate-buffered saline (PBS). The number of viable cells was counted using a Vi-CELL cell viability analyzer.

All experiments were performed using 6-week-old female athymic NCr-*nu/nu* mice purchased from National Cancer Institute Frederick Cancer Research Institute (Bethesda, MD). Nude mice were maintained and used according to institutional guidelines. The experimental protocols were approved by the Institutional Animal Care and Use Committees of University of Louisville (Louisville, KY) and Memorial Sloan-Kettering Cancer Center (New York, NY). Animals were housed five per cage and kept in the institutional small animal facility at a constant temperature and humidity. Food pellets and water were provided *ad libitum*.

Establishment of Tumor Models in Nude Mice

Cancer cell suspensions (5×10^6 cells in 0.1 ml of PBS) were injected intraperitoneally and subcutaneously into unanesthetized mice to generate peritoneal carcinomatosis or subcutaneous xenografts, respectively. Ascites was generally developed and observed to be bloody and contained a distribution of free-floating single cancer cells or cancer cell aggregates (ascites tumors) of sizes up to 1 mm in diameter 4 to 7 weeks after cancer cell inoculation. At these times, distributions of serosal tumors ranging from a few hundred micrometers up to several millimeters in diameter were also present. Subcutaneous xenografts grew to approximately 1 cm in diameter 3 to 4 weeks after cancer cell inoculation into the hind legs.

Experimental Procedures

Ascites pO_2 measurement. Mice were anesthetized by subcutaneous injection of ketamine/xylazine (100 mg/10 mg) combination cocktail (0.2 ml) on the back. A 1-cm incision was carefully made on the peritoneum wall to explore the peritoneal cavity, and ascites pO_2 was measured immediately with an OxyLite probe connected to a four-channel fiber-optic oxygen-sensing device (OxyLite 4000; Oxford Optronix, Oxford, United Kingdom). The OxyLite probes were calibrated by the manufacturer before their delivery. A total of 63 measurements were performed using three mice.

Detection of hypoxia in ascites carcinomas and serosal tumors. In the study, a total of 15 mice, that is 5 mice per cell line, were examined. The exogenous hypoxia marker pimonidazole hydrochloride (1-[(2-hydroxy-3-piperidinyl)propyl]-2-nitroimidazole hydrochloride) (Hypoxyprobe Inc, Burlington, MA) was dissolved in physiological saline at a concentration of 20 mg/ml, and 0.1 ml of the solution was injected through the lateral tail vein 1 hour before animal sacrifice [14]. The blood perfusion marker Hoechst 33342 (Sigma-Aldrich, St Louis, MO) was dissolved in physiological saline at a concentration of 5 mg/ml and 0.1 ml was injected intravenously 1 minute before animal sacrifice [14]. The cellular proliferation marker bromodeoxyuridine (Roche Diagnostics, Indianapolis, IN) first dissolved in DMSO and then in physiological saline (20 mg/ml) was administered through tail vein injection 1 hour before animal sacrifice [14]. In all cases, fresh drug solutions were prepared on the day of injection. Immediately after animal sacrifice, ascites tumors were harvested, washed with cold PBS to remove red blood cells, frozen, and embedded in optimal cutting temperature medium (OCT 4583; Sakura Finetek, Torrance, CA). Serosal tumors were collected and washed with cold PBS to remove any attached ascites tumors before freezing, and immediately thereafter, five contiguous 7-μm-thick tissue sections were cut using a 3050 S cryostat microtome and adhered to poly-L-lysine–coated glass microscope slides.

^{18}F-FDG uptake in ascites carcinomas, serosal tumors, and subcutaneous xenografts. ^{18}F-FDG was purchased from P.E.T. NET Pharmaceuticals Inc (Houston, TX). All animals were fasted overnight before experiments, which were performed without anesthesia. Room air breathing mice were injected through the tail vein with a mixture of ^{18}F-FDG (7.4 MBq) and pimonidazole (2 mg) 1 hour before sacrifice (total injection volume of 0.2

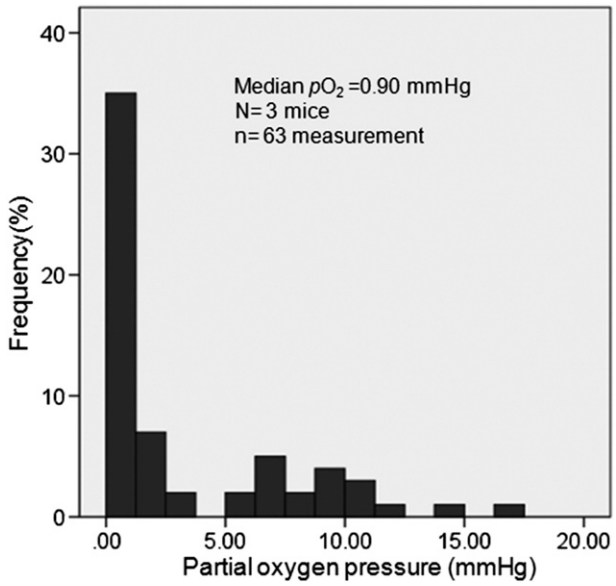

Figure 1. Frequency distributions of measured ascites fluid partial oxygen pressures (pO_2 histograms). Three anesthetized live mice with HT29 ascites carcinomatosis are studied, and a total of 63 measurements are performed.

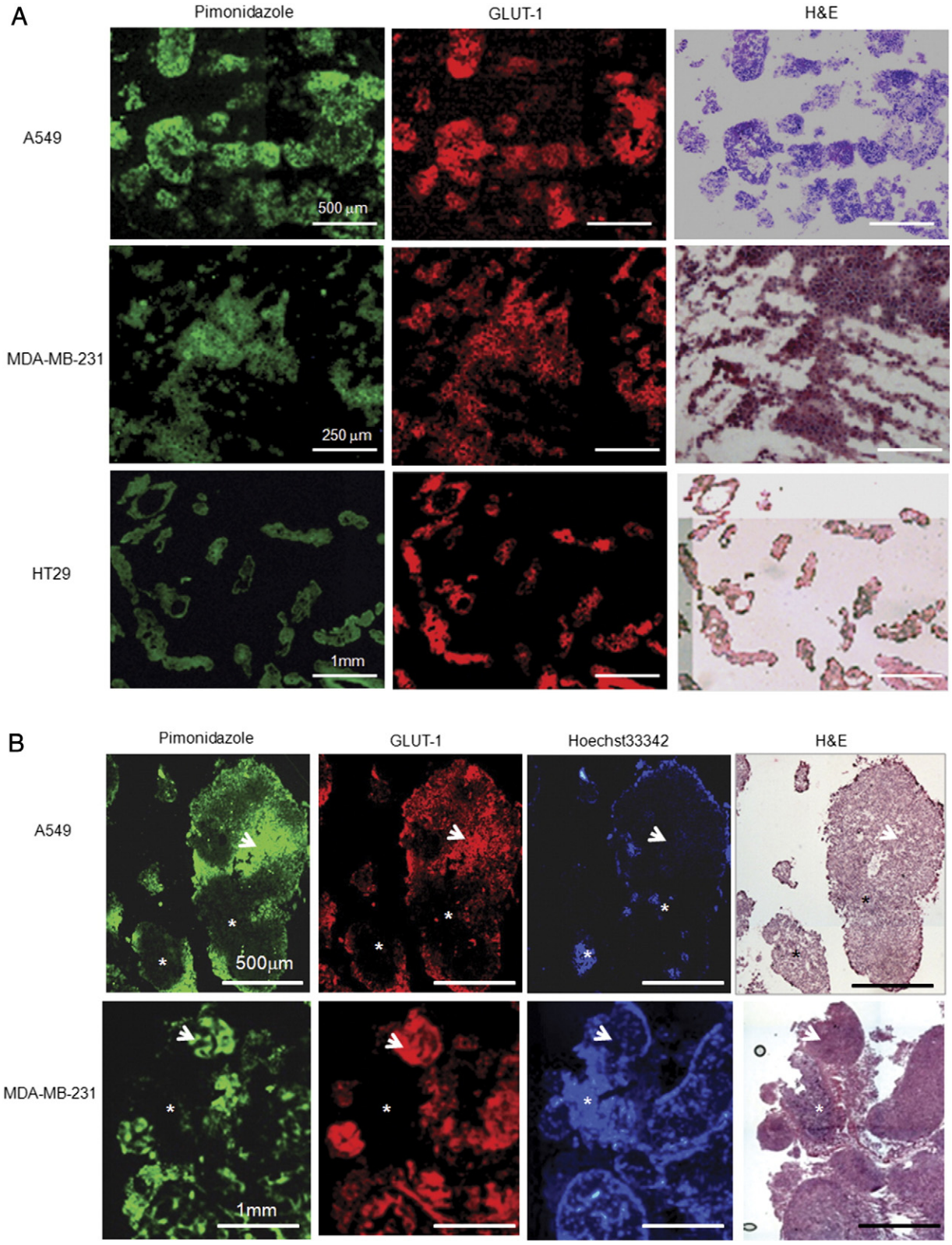

Figure 2. Hypoxia status of ascites carcinoma and peritoneal tumors. (A) A collection of single cancer cell and cancer cell clusters harvested from ascites after intraperitoneal injection of A549, MDA-MB-231, and HT29 cells, respectively, stained positive for pimonidazole and GLUT-1, indicating that all ascites carcinomas are hypoxic. The same frozen section is used for both pimonidazole and GLUT-1 staining (scale bars as indicated). (B) Representative images of A549 and MDA-MB-231 peritoneal tumors that attached to the serosa. Pimonidazole and GLUT-1–stained positive regions (arrow) suggest hypoxia. Regions with Hoechst 33342 binding (asterisk) have low pimonidazole and GLUT-1 fluorescence, indicating normoxic cancer cells. Scale bars are indicated. Hematoxylin and eosin stain from the same or adjacent section is provided for reference.

ml). Hoechst 33342 (0.5 mg, 0.1 ml) was injected through the tail vein 1 minute before sacrifice. A549, HT29, and MDA-MB-231 peritoneal carcinoma and subcutaneous xenograft-bearing mice were studied.

Visualization of Hypoxia, Perfusion, and Proliferation on Tumor Sections

Microscopic images of the distributions of pimonidazole, glucose transporter-1 (GLUT-1), carbonic anhydrase IX (CA9), Hoechst 33342, and bromodeoxyuridine were obtained from the same or adjacent section as described previously [14,16]. Briefly, slides were air-dried, fixed in cold acetone (4°C) for 20 minutes, and incubated with SuperBlock (Pierce Biotechnology, Rockford, IL) at room temperature for 30 minutes. All antibodies were also applied in SuperBlock. Sections were then incubated with fluorescein isothiocyanate–conjugated anti-pimonidazole monoclonal antibody (Hypoxyprobe Inc), diluted 1:25, for 1 hour at room temperature. GLUT-1 staining was performed on the same section by incubating for 1 hour at room temperature with a primary rabbit anti–GLUT-1 polyclonal antibody (Millipore) diluted 1:50, followed by 1 hour at room temperature with either Alexa Fluor 568– (for sections co-stained with pimonidazole) or Alexa Fluor 488–conjugated goat anti-rabbit antibody (1:100; Molecular Probes, Eugene, OR). HT29 tumor sections were co-stained for the hypoxia-regulated protein CA9 by including chimeric anti-CA9 (cG250) antibody (a gift from Dr Gerd Ritter, Ludwig Institute for Cancer Research, New York, NY) at a final concentration of 10 μg/ml. Sections were washed three times in PBS, with each wash lasting 5 minutes. For CA9 staining, sections were then incubated with Alexa Fluor 568–conjugated goat anti-human antibody (1:100; Molecular Probes) and washed again. Due to low expression levels, HCT-8 tumor sections were not stained for CA9. To control for nonspecific binding of the pimonidazole antibody, sections were stained from tumors that had not been exposed to pimonidazole. Controls for GLUT-1 and CA9 staining consisted of sections where primary antibody was omitted.

Proliferation marker bromodeoxyuridine staining was performed on adjacent sections that had been previously imaged for pimonidazole, GLUT-1, or CA9. Sections were treated with 2 N HCl for 10 minutes at room temperature followed by 0.1 M Borax for 10 minutes at room temperature. Sections were then exposed to Alexa Fluor 594–conjugated anti-bromodeoxyuridine antibody (1:20 dilution; Molecular Probes) for 1 hour at room temperature and washed.

Images were acquired using a Nikon Eclipse E800 fluorescence microscope (Nikon America Inc, Melville, NY) equipped with a motorized stage (Ludi Electronic Products Ltd, Hawthorne, NY). Pimonidazole and Hoechst 33342 were imaged using green and blue filters, respectively. CA9 and bromodeoxyuridine were imaged using a red filter. GLUT-1 was imaged using either a red or a green filter dependent on secondary antibody.

^{18}F-FDG Digital Autoradiography

Digital autoradiography (DAR) was obtained by placing the tumor sections in a film cassette against an imaging plate as described previously [9,13,16,17]. The same plate was used throughout the experiments; the plate was exposed for ~20 hours and read by a Cyclone Plus imaging system (PerkinElmer, Inc, Waltham, MA) that generated digital images with pixel dimensions of 42 × 42 μm. DAR images were quantified by the OptiQuant software (PerkinElmer Inc), and tracer uptake was measured as digital light unit per square millimeter (DLU/mm^2), which was converted to MBq/g, based on the known section thickness (7 μm) and the system calibration factor, allowing the results to be expressed as percentage injected dose per gram tumor tissue (%ID/g).

Statistical Analysis

Ascites fluid pO_2 was expressed as median ± SEM, and ^{18}F-FDG uptake was expressed as mean ± SD. Statistical significance was examined by two-tailed Student's *t*-test. A *P* value less than .05 was considered as statistically significant difference.

Results

Ascites fluid pO_2 measured by OxyLite systems was as low as 0.90 ± 0.53 mm Hg (0.12 ± 0.07% O_2, median ± SEM, n = 63 measurements) in three HT29 ascites carcinoma mice (Figure 1). Ascites pO_2 was 0.97 ± 0.68 mm Hg and 1.01 ± 0.55 mm Hg in A549 and MDA-MB-231 ascites carcinoma models, respectively.

For A549, MDA-MB-231, and HT29 cell lines, all single cancer cells and ascites tumors (clusters of pure cancer cells) harvested from ascites fluid were stained positive for both pimonidazole and GLUT-1 (Figure 2*A*), indicating uniform significant hypoxia. In contrast, larger serosal tumors contained normoxic (both pimonidazole and GLUT-1 were negative) and hypoxic (stained positive for pimonidazole and GLUT-1) cancer cells. Representative images from A549 and MDA-MB-231 serosal tumors were presented in Figure 2*B*. Similar pattern was observed in HT29 serosal tumors [14].

In A549 peritoneal tumor model, increased glucose demand detected by ^{18}F-FDG was concurrent with the presence of tumor hypoxia as shown in Figure 3. In room-air breathing mice, hypoxic ascites tumors, submillimeter serosal tumors, and hypoxic portions of larger serosal tumors all had high ^{18}F-FDG uptake (Figure 3*A*). However, normoxic portions of larger serosal tumors had significantly lower ^{18}F-FDG uptake, which was not statistically different from the activity of liver tissue (Figure 3*B*). Similar findings were also observed in HT29 subcutaneous xenograft (Figure 3*C*). ^{18}F-FDG uptake (% ID/g) in hypoxic tissue was significantly higher than normoxic portions of larger A549 serosal tumors ($P < .001$). Of note, ^{18}F-FDG uptake in normoxic cancer cells was not statistically different from the normal liver tissue, stromal tissue, and necrosis ($P > .05$; Figure 3*D*). Results were broadly similar in HT29 and MDA-MB-231 models (data not shown).

^{18}F-FDG uptake and its relationship to tumor hypoxia, blood perfusion, and proliferation were summarized in Figure 4. Representative examples show the relationship between ^{18}F-FDG uptake and pimonidazole, GLUT-1, CA9, bromodeoxyuridine, and Hoechst 33342 in an HT29 subcutaneous xenograft. There was spatial co-localization between high levels of ^{18}F-FDG uptake and high pimonidazole binding and CA9 and GLUT-1 expression. Proliferating cancer cells are generally located in well-perfused (as detected by Hoechst 33342) portions of tumors where cancer cells were normoxic (lack of positive stain of hypoxic markers). Well-perfused and proliferative cancer cells are generally associated with low ^{18}F-FDG accumulation. Similar results were obtained from A549 subcutaneous xenografts that were presented elsewhere [9].

Discussion

The Warburg effect has been considered as a fundamental feature of cancer for more than 80 years, which states that in the presence of ample oxygen, cancer cells use glucose by aerobic glycolysis [1].

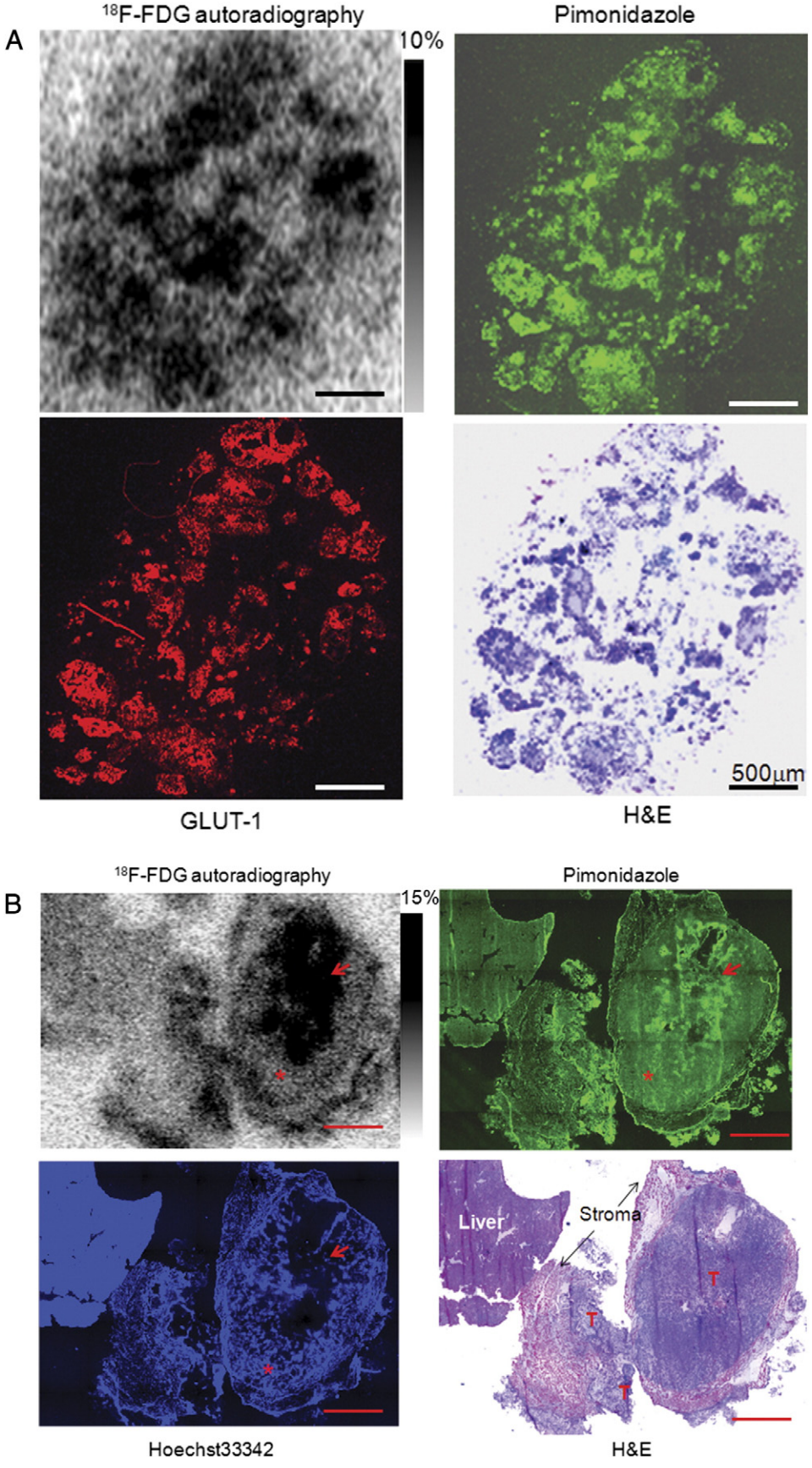
A
18F-FDG autoradiography
Pimonidazole
10%
500μm
GLUT-1
H&E
B
18F-FDG autoradiography
Pimonidazole
15%
Liver
Stroma
T
T
T
Hoechst33342
H&E

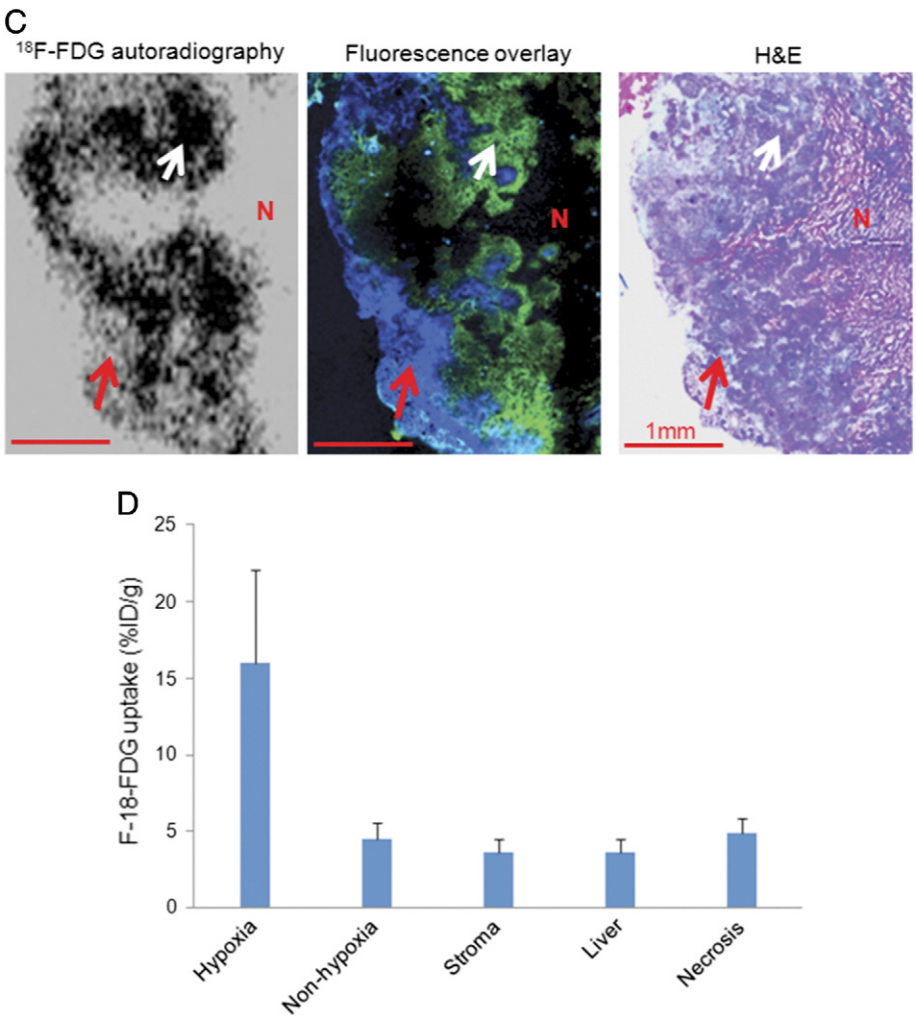

Figure 3. Comparison of ^{18}F-FDG uptake with tumor hypoxia. (A) ^{18}F-FDG uptake and tumor hypoxia in A549 ascites tumors: ascites tumors have high ^{18}F-FDG uptake and high pimonidazole binding and GLUT-1 expression. Scale bar is 500 μm. GLUT-1 imaging was obtained from the adjacent section and all others from the same section. (B) ^{18}F-FDG uptake and tumor hypoxia in A549 serosa tumors: increased ^{18}F-FDG uptake is coincident with high pimonidazole binding and GLUT-1 expression (hypoxia, as indicated by an arrow). Regions of the tumor with negative pimonidazole and GLUT-1 stain but high Hoechst 33342 binding (normoxic regions are marked by asterisks), normal liver, stroma, and necrosis are associated with low ^{18}F-FDG uptake. T, tumor tissue; scale bar, 2 mm. (C) ^{18}F-FDG uptake and tumor hypoxia in HT29 subcutaneous xenograft. High ^{18}F-FDG uptake is coincident with high pimonidazole binding as indicated by a white arrow. Normoxic (red arrow) and necrotic (N) regions are associated with low ^{18}F-FDG uptake; scale bar, 1 mm. Hematoxylin and eosin stain from the same section is provided for reference. (D) Quantitative ^{18}F-FDG uptake based on a collection of intraperitoneal tumors. ^{18}F-FDG uptake is significantly higher in hypoxia regions than non-hypoxic (normoxic) tumor tissue, stroma, necrosis, and normal liver ($P < .001$ to all). Low ^{18}F-FDG uptake in non-hypoxic tumor tissue is not significantly different from stroma, necrosis, and normal liver.

The Warburg effect has been exploited clinically for cancer detection by ^{18}F-FDG PET. In this study, we have revisited ^{18}F-FDG uptake in cancer. Our data present several challenges to the Warburg effect.

We have found that pO_2 of ascites fluid in mice was generally less than 1 mm Hg (Figure 1); therefore, it is not surprising that single cancer cells and clusters of cancer cells were severely hypoxic (Figure 2) [13,14,16,17], and glucose demand measured by ^{18}F-FDG uptake was high (Figure 3). Although this agrees with the increase in glucose demand observed by Warburg, this is unlikely to be due to mitochondrial dysfunction; it has been proven that the mitochondrion of cancer cells is functional [18]. It is, however, probably due to the absence of O_2, preventing oxidative phosphorylation and the generation of adenosine triphosphate (ATP) in the mitochondria. In addition, hypoxia results in the up-regulation of glucose transporters and hexokinase proteins [19-22], key facilitators of glucose uptake and metabolism. Given their hypoxic environment, ascites cancer cells may use anaerobic glycolysis to generate ATP; it is unlikely through "aerobic glycolysis" because of the lack of oxygen. Anaerobic glycolysis is an inefficient biochemical pathway of energy generation and requires significantly more glucose molecules than oxidative phosphorylation to produce lesser amounts of ATP, which induces higher uptake of ^{18}F-FDG in hypoxic cancer cells.

Larger serosal tumors contain relatively well-perfused and normoxic regions, and the glucose demand measured by ^{18}F-FDG is significantly lower than ascites cancer cells (Figure 3) [16], suggesting that high glucose demand is not a general feature of normoxic cancer cells. While normoxic cancer cells had low glucose

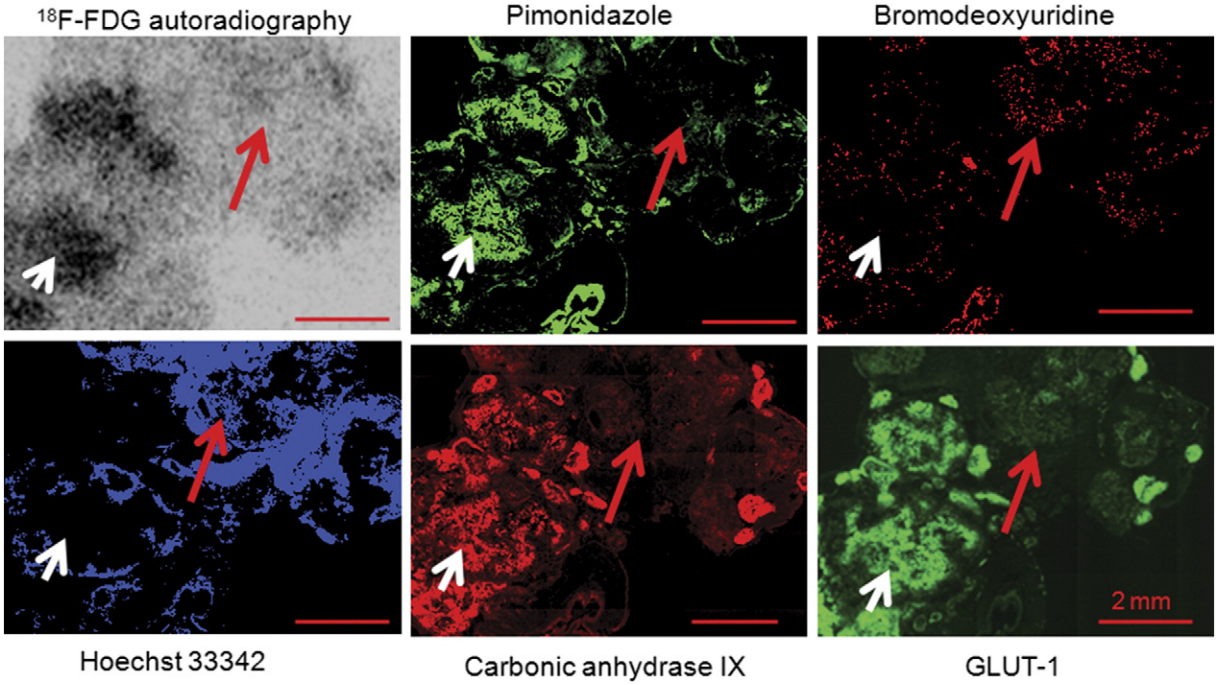

Figure 4. Relationship between ^{18}F-FDG uptake and hypoxia, proliferation, and perfusion in HT29 serosal carcinomatosis. Hypoxic regions, where pimonidazole, GLUT-1, and CA9 are stained positively, have high ^{18}F-FDG uptake (white arrow). Well-perfused regions where Hoechst 33342 is positive and proliferating cancer cells stained positively for bromodeoxyuridine have low ^{18}F-FDG uptake (red arrow). All scale bars are 2 mm.

demand, they presumably have higher energy requirements as they progress through the division cycle, and this energy demand is presumably met by high efficacy oxidative phosphorylation for ATP generation. Of note, normoxic cancer cells have similar levels of ^{18}F-FDG with liver tissue, intratumoral stromal tissue, as well as necrosis. Therefore, low ^{18}F-FDG uptake portion of tumor may not indicate the lack of viable cancer cells.

Proliferation plays an important role in cancer development, cellular proliferation and hypoxia are generally exclusive, and the presence of tumor hypoxia is due to the faster proliferation rate of the cancer cells that are located closer to the functional blood vessels than the "angiogenesis switch". Apparently, cell proliferation requires more energy for the biologic process. Interestingly, proliferating cancer cells in normoxic cancer zones have lower ^{18}F-FDG uptake compared to less proliferative cancer cells that are located in hypoxic zones of a cancerous tumor (Figure 4) [9]. The possible explanation is that proliferating cancer cells generate ATP from glucose, at least to some extent, through high efficacy oxidative phosphorylation therefore requiring less amount of glucose to generate enough energy, in other words, low ^{18}F-FDG accumulation.

In this study, we have mimicked Warburg's experimental conditions by generating ascites carcinomas with colon cancer, breast cancer, and lung cancer cells. Ascites fluid was evident, and ascites tumors and cancer cells were harvested in all the lines we tested. Our findings indicated that ascites fluid, cancer cells, and ascites tumors floating in it were severely hypoxic. Hypoxic ascites carcinomas and submillimeter serosal tumors had higher glucose demand than less hypoxic larger serosal tumors generated from the same cancer cell lines. This pattern is cell line independent, and as we tested lung cancer cell line A549, breast cancer cell line MDA-MB-231, and colon cancer cell line HT29, the results were broadly similar.

^{18}F-FDG PET-CT scans based on the Warburg effect has been widely used for cancer detection and therapy response [23-25]. The success of such utilization is not surprising, because most solid malignancies have increased ^{18}F-FDG, as hypoxia is a feature of most solid cancers [26-31]. However, it is also likely that the presence of associated low ^{18}F-FDG activities of some tumors or tumor regions [10,11] is probably due to a lack of hypoxia in such tumors or regions of the tumors. Negative ^{18}F-FDG uptake does not necessarily mean benign disease.

In both primary lesion and metastases of patients with NSCLC, Beer et al. [12] demonstrated a mismatched pattern of intratumoral distribution of ^{18}F-FDG and ^{18}F-galacto-RGD, that is, ^{18}F-FDG did not accumulate as much in well-perfused regions of the tumor identified by increased ^{18}F-galacto-RGD, which binds to the $\alpha_v\beta_3$ expressed by endothelial cells. Therefore, in patients, well-perfused cancer tissue is associated with low ^{18}F-FDG uptake or low glucose demand. Accordingly, assumptions in ^{18}F-FDG PET interpretations for cancer management should be reconsidered because low ^{18}F-FDG uptakes in tumor following treatment may not necessarily mean the absence of viable cancer cells.

^{18}F-FDG preferentially accumulates in hypoxic cancer cells, and 3′-deoxy-3′-^{18}F-fluorothymidine accumulates mostly in proliferative cancer cells, which are usually not hypoxic [7,9]. We have recently proposed that the combination of ^{18}F-FDG and 3′-deoxy-3′-^{18}F-fluorothymidine with single PET imaging would give a more accurate representation of viable tumor tissue volume than a PET image obtained with either tracer alone [32].

We emphasize here that the DAR signal of ^{18}F-FDG is directly contributed by positrons and not gamma photons. In a pilot study, we have inserted a piece of blanket poly-L-lysine–coated glass microscope between the plate and the tumor section slide, and

most ^{18}F-FDG signals were shielded, indicating the role of the positron in ^{18}F-FDG autoradiography. We are confident that the spatial correlation between ^{18}F-FDG autoradiography and immunohistochemical staining photos presented in this article is true.

Conclusion

In the mouse model of ascites carcinoma, ascites and floating ascites carcinomas are severely hypoxic, contradicting the assumed ample oxygen condition of the Ehrlich ascites carcinoma model in which the "Warburg effect" was derived from. Glucose utilization measured by ^{18}F-FDG uptake increases in hypoxic but not normoxic cancer cells, posing a challenge for the conventional Warburg effect. The knowledge enriches the better understanding of ^{18}F-FDG in oncology application.

Acknowledgments

This study was supported, in part, by Kentucky Lung Cancer Research Program Award (cycle 9) and National Institute of Health grant R01 CA84596. The authors have no conflict of interest relevant to this article.

References

[1] Warburg O (1956). On the origin of cancer cells. *Science* **123**, 309–314.
[2] Vander Heiden MG, Cantley LC, and Thompson CB (2009). Understanding the Warburg effect: the metabolic requirements of cell proliferation. *Science* **324**, 1029–1033.
[3] Clavo AC, Brown RS, and Wahl RL (1995). Fluorodeoxyglucose uptake in human cancer cell lines is increased by hypoxia. *J Nucl Med* **36**, 1625–1632.
[4] Burgman P, O'Donoghue JA, Humm JL, and Ling CC (2001). Hypoxia-induced increase in FDG uptake in MCF7 cells. *J Nucl Med* **42**, 170–175.
[5] Hara T, Bansal A, and DeGrado TR (2006). Effect of hypoxia on the uptake of [methyl-^{3}H]choline, [1-^{14}C] acetate and [^{18}F]FDG in cultured prostate cancer cells. *Nucl Med Biol* **33**, 977–984.
[6] Busk M, Horsman MR, Jakobsen S, Bussink J, van der Kogel A, and Overgaard J (2008). Cellular uptake of PET tracers of glucose metabolism and hypoxia and their linkage. *Eur J Nucl Med Mol Imaging* **35**, 2294–2303.
[7] Pugachev A, Ruan S, Carlin S, Larson SM, Campa J, Ling CC, and Humm JL (2005). Dependence of FDG uptake on tumor microenvironment. *Int J Radiat Oncol Biol Phys* **62**, 545–553.
[8] Busk M, Horsman MR, Kristjansen PE, van der Kogel AJ, Bussink J, and Overgaard J (2008). Aerobic glycolysis in cancers: implications for the usability of oxygen-responsive genes and fluorodeoxyglucose-PET as markers of tissue hypoxia. *Int J Cancer* **122**, 2726–2734.
[9] Huang T, Civelek AC, Li J, Jiang H, Ng CK, Postel GC, Shen B, and Li XF (2012). Tumor microenvironment–dependent ^{18}F-FDG, ^{18}F-fluorothymidine, and ^{18}F-misonidazole uptake: a pilot study in mouse models of human non–small cell lung cancer. *J Nucl Med* **53**, 1262–1268.
[10] Cheran SK, Nielsen ND, and Patz Jr EF (2004). False-negative findings for primary lung tumors on FDG positron emission tomography: staging and prognostic implications. *AJR Am J Roentgenol* **182**, 1129–1132.
[11] Iwano S, Ito S, Tsuchiya K, Kato K, and Naganawa S (2013). What causes false-negative PET findings for solid-type lung cancer? *Lung Cancer* **79**, 132–136.
[12] Beer AJ, Lorenzen S, and Metz S, et al (2008). Comparison of integrin $\alpha_v\beta_3$ expression and glucose metabolism in primary and metastatic lesions in cancer patients: a PET study using ^{18}F-galacto-RGD and ^{18}F-FDG. *J Nucl Med* **49**, 22–29.
[13] Huang T, Civelek AC, Zheng H, Ng CK, Duan X, Li J, Postel GC, Shen B, and Li XF (2013). ^{18}F-misonidazole PET imaging of hypoxia in micrometastases and macroscopic xenografts of human non-small cell lung cancer: a correlation with autoradiography and histological findings. *Am J Nucl Med Mol Imaging* **3**, 142–153.
[14] Li XF, Carlin S, Urano M, Russell J, Ling CC, and O'Donoghue JA (2007). Visualization of hypoxia in microscopic tumors by immunofluorescent microscopy. *Cancer Res* **67**, 7646–7653.
[15] Li XF and O'Donoghue JA (2008). Hypoxia in microscopic tumors. *Cancer Lett* **264**, 172–180.
[16] Li XF, Ma Y, Sun X, Humm JL, Ling CC, and O'Donoghue JA (2010). High ^{18}F-FDG uptake in microscopic peritoneal tumors requires physiologic hypoxia. *J Nucl Med* **51**, 632–638.
[17] Li XF, Sun X, Ma Y, Suehiro M, Zhang M, Russell J, Humm JL, Ling CC, and O'Donoghue JA (2010). Detection of hypoxia in microscopic tumors using ^{131}I-labelediodo-azomycin galactopyranoside (^{131}I-IAZGP) digital autoradiography. *Eur J Nucl Med Mol Imaging* **37**, 339–348.
[18] Bertout JA, Patel SA, and Simon MC (2008). The impact of O_2 availability on human cancer. *Nat Rev Cancer* **8**, 967–975.
[19] Macheda ML, Rogers S, and Best JD (2005). Molecular and cellular regulation of glucose transporter (GLUT) proteins in cancer. *J Cell Physiol* **202**, 654–662.
[20] Yasuda S, Arii S, and Mori A, et al (2004). Hexokinase II and VEGF expression in liver tumors: correlation with hypoxia-inducible factor 1α and its significance. *J Hepatol* **40**, 117–123.
[21] Wyatt E, Wu R, Rabeh W, Park HW, Ghanefar M, and Ardehali H (2010). Regulation and cytoprotective role of hexokinase III. *PLoS One* **5**, e13823.
[22] Gwak GY, Yoon JH, Kim KM, Lee HS, Chung JW, and Gores GJ (2005). Hypoxia stimulates proliferation of human hepatoma cells through the induction of hexokinase II expression. *J Hepatol* **42**, 358–364.
[23] Lheureux S, Lecerf C, Briand M, Louis MH, Dutoit S, Jebahi A, Giffard F, Fournier CB, Batalla A, and Poulain L, et al (2013). ^{18}F-FDG is a surrogate marker of therapy response and tumor recovery after drug withdrawal during treatment with a dual PI3K/mTOR inhibitor in a preclinical model of cisplatin-resistant ovarian cancer. *Transl Oncol* **6**, 586–595.
[24] Kayed H, Meyer P, He Y, Kraenzlin B, Fink C, Gretz N, Schoenberg SO, and Sadick M (2012). Evaluation of the metabolic response to cyclopamine therapy in pancreatic cancer xenografts using a clinical PET-CT system. *Transl Oncol* **5**, 335–343.
[25] Honer M, Ebenhan T, Allegrini PR, Ametamey SM, Becquet M, Cannet C, Lane HA, O'Reilly TM, Schubiger PA, and Sticker-Jantscheff M, et al (2010). Anti-angiogenic/vascular effects of the mTOR inhibitor everolimus are not detectable by FDG/FLT-PET. *Transl Oncol* **3**, 264–275.
[26] Thomlinson RH and Gray LH (1955). The histological structure of some human lung cancers and the possible implications for radiotherapy. *Br J Cancer* **9**, 539–549.
[27] Li XF, Jiang H, Ma Y, Huang T, Yin X, Civelek AC, and Shen B (2013). A model system for PET radiopharmaceuticals validation: focusing on tumor microenvironment. *Int J Med Phys Clin Eng Radiat Oncol* **2**, 19–29. http://dx.doi.org/10.4236/ijmpcero.2013.21004.
[28] Vaupel P, Schlenger K, Knoop C, and Höckel M (1991). Oxygenation of human tumors—evaluation of tissue oxygen distribution in breast cancers by computerized O_2 tension measurements. *Cancer Res* **51**, 3316–3322.
[29] Nordsmark M, Overgaard M, and Overgaard J (1996). Pretreatment oxygenation predicts radiation response in advanced squamous cell carcinoma of the head and neck. *Radiother Oncol* **41**, 31–39.
[30] Li XF, Ma Y, and Jiang H (2012). Understanding hypoxia microenvironment of micro-metastases. *J Solid Tumors* **2**(2), 28–33.
[31] Brizel DM, Sibley GS, Prosnitz LR, Scher RL, and Dewhirst MW (1997). Tumor hypoxia adversely affects the prognosis of carcinoma of the head and neck. *Int J Radiat Oncol Biol Phys* **38**, 285–289.
[32] Li XF, Huang T, Jiang H, Wang X, Shen B, Wang X, Ng CK, and Civelek AC (2013). Combined injection of ^{18}F-fluorodeoxyglucose and 3′-deoxy-3′-^{18}F-fluorothymidine PET achieves more complete identification of viable lung cancer cells in mice and patients than individual radiopharmaceutical: a proof-of-concept study. *Transl Oncol* **6**, 755–783.